9-1990

Molecular-Diffusive Effects in Penetrative Convection

H. J.S. Fernando
Arizona State University

Leigh J. Little
The College at Brockport, llittle@brockport.edu

Citation/Publisher Attribution:
H.J.S. Fernando and L. J. Little. "Molecular-diffusive Effects in Penetrative Convection," *Physics of Fluids A* 2(1990): 1592-1598. Available on publisher's site at http://link.aip.org/link/doi/10.1063/1.857566.

Molecular-diffusive effects in penetrative convection

H. J. S. Fernando and L. J. Little
Department of Mechanical and Aerospace Engineering, Arizona State University, Tempe, Arizona 85287-6106

(Received 31 January 1990; accepted 17 May 1990)

An experimental study was performed to investigate the influence of molecular diffusion on turbulent entrainment during penetrative convection. The entrainment coefficient E was determined as a function of the Richardson number Ri and Peclet number Pe. It appears that, in parameter ranges $65 < \mathrm{Ri} < 150$ and $10^3 < \mathrm{Pe} < 10^4$, E is a function of Ri, independent of Pe, which indicates inertial-buoyancy dominated mixing and the unimportance of molecular diffusive effects. At high interfacial stabilities, $30 < \mathrm{Ri} < 300$, the entrainment law was found to be given by $E \sim \mathrm{Ri}^{-1}$.

I. INTRODUCTION

The penetration of a convectively driven mixed layer into a nonturbulent, stably stratified layer, owing to mixing at the interface separating them, is called penetrative convection. Because of its relevance in describing many geophysical phenomena, such as the growth of the atmospheric daytime boundary layer against the stable stratification at the tropopause, and the deepening of upper-ocean mixed layer as a result of surface cooling, evaporation or rejection of brine during surface freezing, extensive research efforts have been directed toward understanding physical processes governing penetrative convection. To this end, laboratory experiments have been a very useful tool, because of their ability to elucidate entrainment mechanisms while eliminating (or controlling) undesirable complications such as horizontal advection, radiative and evaporative processes, and large-scale effects. In spite of their contributions to the basic understanding of penetrative convection, the findings of laboratory experiments have left unresolved questions of their applicability to large-scale processes.

A number of laboratory experiments on penetrative convection have been reported. Some of them have dealt with the structure of turbulence in convectively driven mixed layers.[1–3] These studies have established that the rms horizontal velocity u and the integral length scale of turbulence l in the bulk of the mixed layer are scaled by the convective velocity w_* and the depth of the mixed layer h, respectively. Here w_* is defined as $w_* = (q_0 h)^{1/3}$, where $q_0 = g\alpha Q/\rho_0 c_p$ is the buoyancy flux at the heating surface corresponding to a heat flux Q, g is the gravitational acceleration, α is the coefficient of thermal expansion, ρ_0 is a reference density, and c_p is the specific heat. Another category of experiments has considered the entrainment at turbulent–nonturbulent (entrainment) interfaces.[4–7] The entrainment mechanism is conjectured to be the impingement of mixed-layer eddies on the density interface to cause "dome-shaped" and somewhat isolated distortions at the interface; the edges of these domes take the form of inward cusps through which the nonturbulent fluid streams erratically into the turbulent layer.[8] The normalized entrainment rate was evaluated as a function of the Richardson number Ri, which is the sole nondimensional parameter that determines the rate of entrainment if the interfacial mixing is controlled by inertia forces of turbulence and buoyancy forces of the stratification.

If the one-dimensional problem of heating a linearly (temperature) stratified fluid from below with a constant heat flux is considered (Fig. 1), it is easily shown that the rate of entrainment $u_e = dh/dt$ where t is the time, can be written as

$$u_e = f_1(N^2, q_0, h, k_h, \nu), \tag{1}$$

where N is the stability frequency of the stratification, $f_1, f_2, \ldots$ are used to denote functions; and k_h and ν are the molecular diffusivities of heat and momentum, respectively. An alternative form of (1) is

$$u_e/w_* = f_2(\mathrm{Ri}, \mathrm{Pe}, \mathrm{Re}), \tag{2}$$

where $\mathrm{Ri} = N^2 h^2/w_*^2$ is the Richardson number, $\mathrm{Pe} = w_* h/k_h$ is the Peclet number, $\mathrm{Re} = w_* h/\nu$ is the Reynolds number, and u_e/w_* is the entrainment coefficient E. If molecular-diffusive effects are considered to be unimportant because of strong turbulent mixing, then (2) takes the form

$$u_e/w_* = f_3(\mathrm{Ri}). \tag{3}$$

It is clear that the influence of molecular diffusion becomes unimportant at sufficiently large Re and Pe ($= \mathrm{Re}\,\mathrm{Pr}$, where $\mathrm{Pr} = \nu/k_h$ is the Prandtl number), but their critical values above which the molecular-diffusive effects completely disappear are not known. According to Breidenthal and Baker,[9] the turbulence within the interfacial mixing region is well developed when the Reynolds

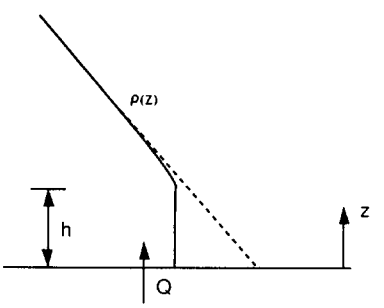

FIG. 1. An idealized experimental configuration: heating of a linearly (temperature) stratified fluid from below with a constant heat flux. Here $\rho(z)$ represents the density distribution resulting from temperature.

 0899-8213/90/091592-05$02.00

number, based on the interfacial shear-layer thickness δ, exceeds about 10^3. Assuming that $\delta \approx 0.1$ h, it is possible to estimate $\mathrm{Re} \approx 10^4$ and $\mathrm{Pe} \approx 10^5$ as the critical values. These predictions are yet to be verified experimentally.

The results of previous experiments carried out to verify (3) have not been able to provide a unified consensus on the functional form of (3). Even though the results of the experiments of Deardorff *et al.*[7] indicate support for the form

$$u_e/w_* \sim \mathrm{Ri}^{-1}, \tag{4}$$

their data are somewhat scattered and the possibility of other types of power laws cannot be ruled out. Breidenthal and Baker[9] suggested that the reason for this scatter may be the involvement of molecular-diffusive effects in the entrainment process, notwithstanding that such an assertion has been discounted by Deardorff *et al.*[7] The data of previous experiments, however, are not extensive enough to check the importance of molecular-diffusive effects in penetrative convection in different Richardson-number regimes. The aim of the present experiments is to address this particular matter. The approach is to determine the dependence of nondimensional parameters that signify molecular-diffusive effects (such as Pe) on the entrainment coefficient.

II. EXPERIMENT

The experiment was designed to provide a flow configuration similar to that is shown in Fig. 1. The test cell is a cubic Plexiglas (1.2 cm thick) tank of linear dimension 0.65 m; see Fig. 2. The bottom of the tank is constructed from 1.2 cm aluminum plate; suitable heating pads (Watlow) and a 7.5 cm thick layer of insulation were placed below this plate. The sides of the experimental apparatus were insulated with a 5 cm layer of styrofoam insulation, sections of which were detachable for flow visualization. The rate of heat input to the tank Q was controlled by adjusting the voltage across the heating elements with a rheostat. For a given rheostat setting, Q was determined by measuring the rate of rise of temperature of a given amount of fresh water contained in the tank, as in Fernando.[10]

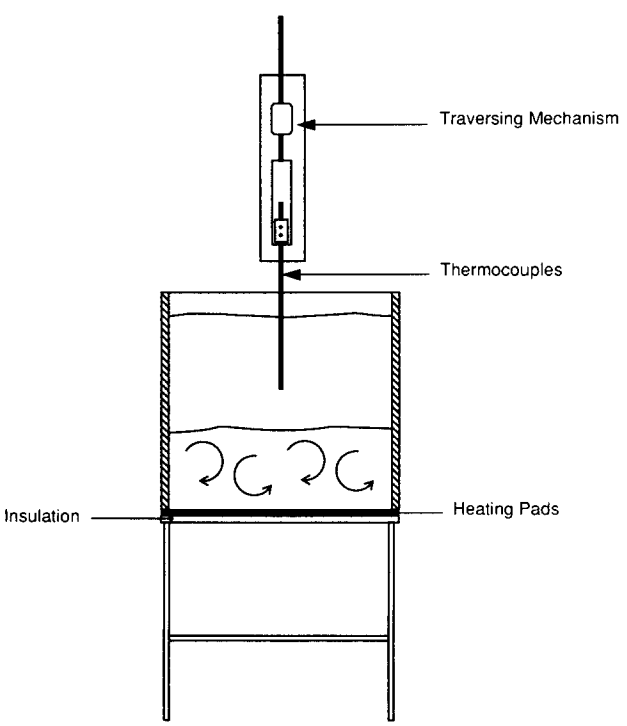

FIG. 2. A schematic diagram of the experimental apparatus.

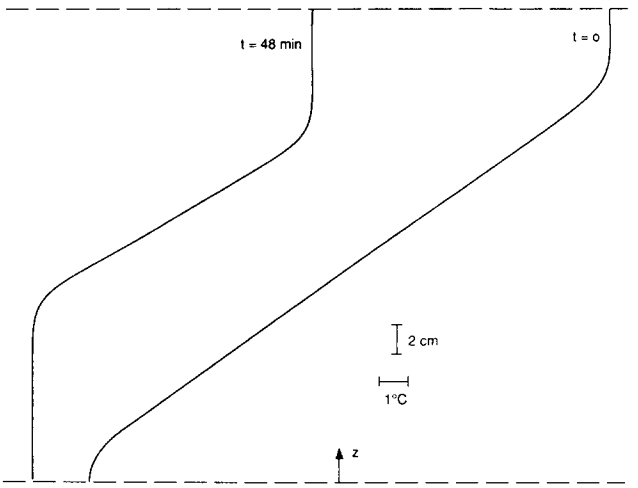

FIG. 3. Two representative temperature profiles taken during an experiment with $q_0 = 4.2 \times 10^{-3}$ m^2 sec^{-3} and $N = 0.40$ sec^{-1}. The time t at which the profile was taken and the scales of the plot are also indicated in the figure.

The linear temperature stratification within the tank was obtained by filling it with layers of hot and cold water of equal thicknesses and then agitating the fluid system using a rake of glass rods to produce vertical mixing. The resulting partially mixed fluid was allowed to equilibrate for about 5 min, after which the temperature profile corresponding to $t = 0$ was taken. A sensitive thermocouple attached to a stepper-motor-driven platform, that traverses with a speed of 1 cm sec^{-1}, was used to determine this profile. A typical initial temperature profile is shown in Fig. 3.

The experiments were started by initiating the heat input and then monitoring the development of the mixed layer by taking temperature profiles at specific time intervals (usually 2 min). Flow visualization was performed by illu-

FIG. 4. A photograph taken using argon-ion laser-sheet flow visualization. The lower convecting layer is added with fluorescein dye. (a) An overturning event caused by high horizontal velocities of the eddies sloshing over the interface. (b) An inward (toward the turbulent layer) cusp of nonturbulent fluid, possibly caused by the eddies impinging adjacent to each other.

minating a section of the test cell using a sheet of argon-ion laser light. A small amount of Fluorescein dye was added to the convective mixed layer, which, when exposed to laser light, fluoresces with a light green color. Figure 4 shows a typical view of the flow obtained using this technique.

During the experiments a mixed layer develops near the heating surface, followed by a constant temperature-gradient layer above it. Near the free surface, the temperature gradient tends to zero, owing to the no-flux boundary condition and resulting from evaporation. The isothermal layer close to the heating surface was defined as the mixing layer. The stably stratified layer above the mixed layer acts as an obstruction to the propagating turbulent front. The temperature gradient of this layer dT/dz was converted to the stability frequency N using $N^2 = g\alpha\, dT/dz$. The mixed-layer height h versus time t data were curve fit and were differentiated to calculate the entrainment rate u_e.

The major uncertainty of the experiment is associated with the measurement of h. The entrainment interface is often distorted and the measurement of h using a vertical temperature profile taken at a particular location may not represent the exact mean mixed-layer height. The accuracy of the measurements thus depends on the amplitude of the wave oscillations, and hence on Ri. According to Crapper and Linden,[11] however, at high Richardson numbers, the instantaneous and mean mixed-layer heights do not differ substantially. Further it is expected that the errors resulting from interfacial distortions are corrected, to a certain extent, by curve fitting of data to obtain a smooth T-z profile. The estimated uncertainties are $\pm$ 10% for h; $\pm$ 15% for u_e; $\pm$ 0.2 K for temperature; $\pm$ 5% for q_0; and $\pm$ 1 sec for t.

III. EXPERIMENTAL RESULTS

Qualitative observations: Flow-visualization studies indicate that mixing at the interface, at Richardson numbers greater than about 30, takes place as a result of local instabilities caused by the impingement of eddies on the interface. At lower Richardson numbers, turbulent eddies tend to engulf nonturbulent fluid, as occurs in homogeneous fluids. As pointed out by Hannoun *et al.*,[12] when the energy-containing eddies impinge on strong density interfaces, they tend to flatten, thereby transferring the kinetic energy of the vertical component to horizontal ones. This intercomponent energy transport produces comparatively high horizontal velocities along the interface that can generate overturning billows [Fig. 4(a)]. Further, if two energy-containing eddies impinge at nearby locations, their combined influence can cause inward cusps, thus forcing nonturbulent fluid into the mixed layer [Fig. 4(b)]. Another possible mixing mechanism at shear-free density interfaces is the breaking of interfacial waves.[12] In the present experiments, however, such events were not evident. As pointed out by Narimousa and Fernando,[13] the rapid decay of excited internal waves in heat-stratified fluids may be the cause for the absence of wave breaking.

Quantitative measurements: Figure 5 shows a plot of the entrainment coefficient versus Richardson number for several experimental runs. Although there is a certain amount of scatter, for the range $30 < \mathrm{Ri} < 300$, the data can be well

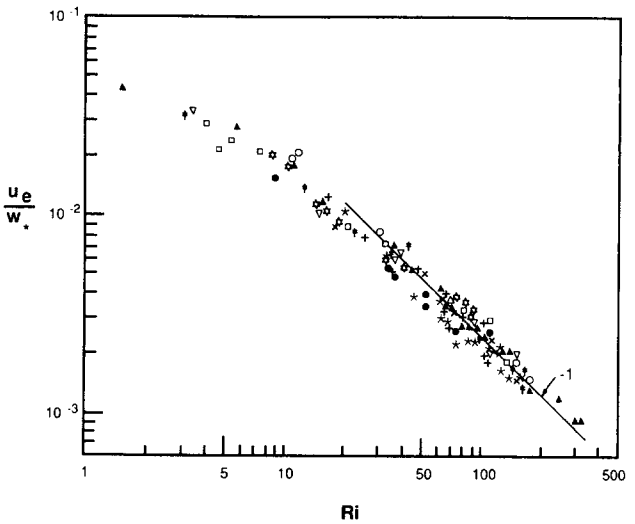

FIG. 5. A log–log graph of u_e/w_* vs Ri. Different symbols indicate different experimental runs. The ranges of parameters used for these runs are $0.2\ \mathrm{sec}^{-1} < N < 0.9\ \mathrm{sec}^{-1}$, $3.84\times10^{-7}\ \mathrm{m^2\,sec^{-3}} < q_0 < 2.62\times10^{-6}\ \mathrm{m^2\,sec^{-3}}$.

represented by a power law of the form $E\alpha\ \mathrm{Ri}^{-1}$, with a proportionality constant of 0.2. At low Ri, u_e/w_* appears to approach a value of about 0.05, indicating that the entrainment mechanism is independent of Ri. At low Ri, the mixed-layer eddies are sufficiently energetic to engulf fluid from the stratified layer, as if there were no buoyancy effects.[14,15] In order to check whether the entrainment coefficient is dependent on molecular parameters, it is possible to recast (2) in the form

$$u_e/w_* = f_4(\mathrm{Ri}, \mathrm{Pe}, \mathrm{Pr}), \tag{5}$$

where $\mathrm{Pr} = \nu/k_h$ is the Prandtl number. During the course of the experiments, the variation of Pr was small and thus it is possible to expect u_e/w_* to depend only on Ri and Pe of the flow. The dependence of E on Pe was evaluated while Ri was being held approximately constant; the results, for several such Ri values, are given in Figs. 6(a)–6(e). The u_e/w_* vs Pe data for each Ri were curve fit to a power law of the form $u_e/w_* = A\ \mathrm{Pe}^{-n}$, using regression analysis, and the results are given in Table I. The parameters ranges used were $10 < \mathrm{Ri} < 200$ and $10^3 < \mathrm{Pe} < 10^4$. Overall low values of n and the correlation coefficient suggest that E may be independent of Pe, but the data taken at $\mathrm{Ri} < 65$ indicate that the possibility of a weak dependence of E on Pe cannot be ruled out. The latter experiments cover the parameter range $800 < \mathrm{Pe} < 9000$. As noted before, the entrainment data at low Ri are subjected to higher uncertainty and hence definitive conclusions cannot be made based on such data.

IV. SUMMARY AND DISCUSSION

The purpose of the present work was to investigate whether molecular-diffusive effects play an important role in the turbulent entrainment across a heat-stratified interface induced by convective turbulence. In explaining the scatter of the entrainment data of Deardorff *et al.*,[7] Breidenthal and Baker[9] have invoked the effects of molecular diffusion; ac-

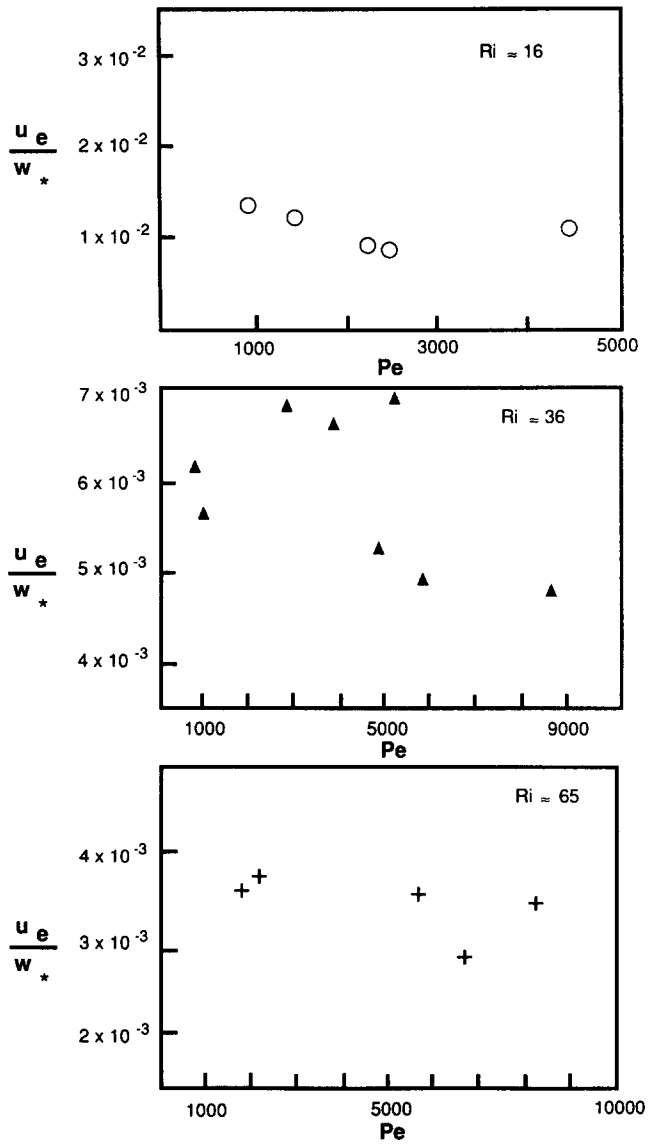

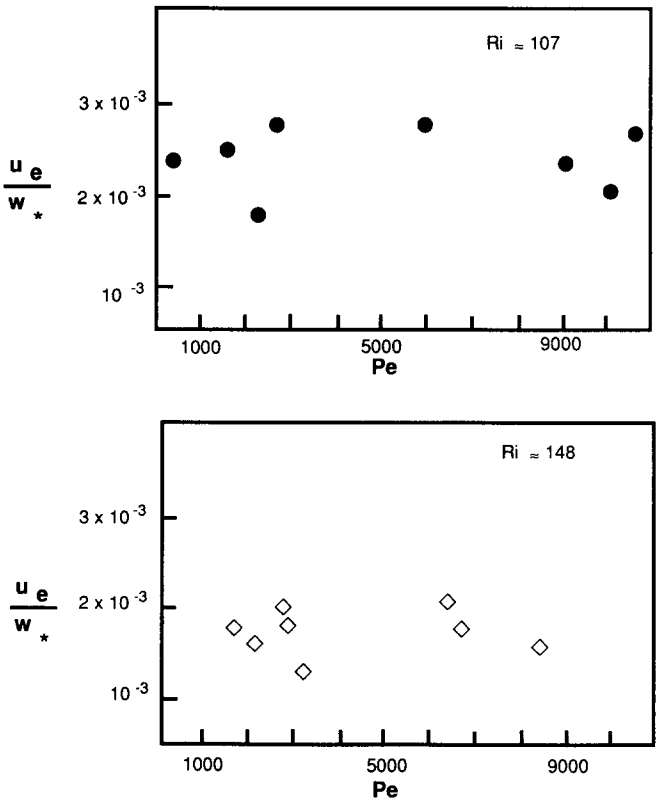

FIG. 6. Plots of u_e/w_* vs Pe, evaluated at approximately constant Ri. The average Ri for each case is shown in the upper right-hand corner.

cordingly, a strong Peclet number dependence of the entrainment coefficient can be expected when the Reynolds number is less than about 10^4. Since $\mathrm{Re} = \mathrm{Pe}\,\mathrm{Pr}^{-1}$ and $\mathrm{Pr} \approx 5$–7, it is clear that, for most of the experimental runs reported in this paper, the criterion $\mathrm{Re} < 10^4$ is satisfied. Nonetheless, no significant dependence of u_e/w_* on Pe could be identified, especially when $\mathrm{Re} > 65$. Although the experiments corresponding to $\mathrm{Ri} \approx 36$ and 16 indicate a possible weak dependence of E on Pe, the results need to be interpreted with caution because of the large uncertainties of the measurements at small Ri. It is recommended that, in future studies, improved measurement techniques, capable of providing ensemble-averaged mixed-layer thicknesses, be used in order to reduce the uncertainties.

TABLE I. The results of a regression analysis of entrainment data taken at a given Ri but at different Pe.

Ri[a]	Pe dependence $u_e/w_* = A\,\mathrm{Pe}^{-n}$		Correlation coefficient
	A	n	
148 (6.0)	1.30×10^{-3}	0.003	−0.011
107 (4.5)	2.60×10^{-3}	0.012	−0.054
65 (1.7)	2.62×10^{-3}	−0.040	0.225
36 (3.0)	1.15×10^{-2}	0.085	−0.400
16 (2.3)	5.64×10^{-2}	0.215	−0.628

[a] In practice it is difficult to obtain data repeatedly at a given Ri. Thus, in the calculations, an ensemble of data clustered around the given Ri, with a standard deviation indicated in the parentheses, was used.

The results show that, for $30 < \mathrm{Ri} < 300$, the entrainment law can be represented by $u_e/w_* = 0.2\,\mathrm{Ri}^{-1}$. The scatter in the u_e/w_* vs Ri data of Deardorff *et al.*[7] may thus be due to some other reason. One possible cause is the use of a rather tenuous process in calculating the mixed-layer height and buoyancy jump Δb across the interface. They used the height at which the buoyancy flux takes its most negative value as the average mixed-layer height. In calculating the buoyancy flux, an integral form of the buoyancy conservation equation was used. Cumulative errors associated with such calculations may have contributed to the observed scat-

ter. In the present work, a simpler definition was used for h and the difficulties associated with evaluating Δb were eliminated by using the instantaneous buoyancy frequency N to specify the buoyancy forces encountered by the eddies.

According to (5), besides Ri and Pe, Pr (or generally, the Schmidt number $\mathrm{Sc} = \nu/k$, where k is the molecular diffusivity of the stratifying agent) can also affect the entrainment process. In the present study Sc was not changed appreciably to observe such a dependence, but the penetrative-convection studies of Kantha,[6] which were performed using salinity-stratified fluids and unstable (saline) buoyancy fluxes, indicate that the Schmidt number effects may not be important.

The Richardson numbers corresponding to the atmosphere vary over a wide range, including the range covered in the present study. For example, for typical parameters of a growing convective layer with moderate stratification, $w_* \approx 1.5\ \mathrm{m\ sec^{-1}}$, $h \approx 100$ m and $N \approx 0.1\ \mathrm{sec^{-1}}$ (1 cycle/min), the value $\mathrm{Ri} \approx 45$ is obtained. The atmospheric Peclet numbers, however, are much higher; for the above example, $\mathrm{Pe} \approx 8 \times 10^8$. The present results indicate that Pe effects can be unimportant for $10^3 < \mathrm{Pe} < 10^4$, but obviously this range can be extended to encompass higher Pe values in view of the weakening influence of molecular-diffusive effects with increasing Pe. Thus it is clear that, at least for the Ri range covered, the present results should have applicability to atmospheric situations.

Finally, it should be noted that a number of studies have been devoted to investigate the influence of molecular diffusion on mixing across density interfaces caused by mechanically induced turbulence; reviews in this context can be seen in Phillips[14] and Turner.[15] Phillips[14] argued that the entrainment in sheared density interfaces should become completely molecular-diffusion dominated when Ri exceeds a critical value Ri_c, where $\mathrm{Ri}_c \simeq \mathrm{Pe}\ E$. Some implicit support for this prediction has been provided by the experiments of Narimousa *et al.*[16] In the context of oscillating-grid induced shear-free turbulence, Turner[17] reported that the entrainment laws corresponding to heat and salt-stratified fluids take the forms $E \sim \mathrm{Ri}^{-1}$ and $E \sim \mathrm{Ri}^{-3/2}$, respectively; since both types of experiments have been carried out in the same range of Reynolds number ($ul/\nu \sim 30$), the only difference between the experiments were the difference in molecular diffusivities of heat and salt. Further, based on dimensional arguments, Turner[17] conjectured that the general entrainment law can be written as $E \sim \mathrm{Ri}^{-1}(c + \mathrm{Ri\ Pe})^{-1/2}$, where c is a constant: Based on the results of further experiments, this expression has been modified by Hopfinger and Toly[18] as $E \sim \mathrm{Ri}^{-3/2}(c_1 + c_2\,\mathrm{Ri}^{1/2}\,\mathrm{Pe}^{-1/2})$, where c_1 and c_2 and constants, so that $E \sim \mathrm{Ri}^{-3/2}$ and $E \sim \mathrm{Ri}^{-1}\,\mathrm{Pe}^{-1/2}$ represent the entraiment laws at high and low Peclet numbers, respectively. Although the penetrative convection studied here falls into the category of shear-free turbulence, the entrainment data do not follow the above-mentioned entrainment law. Recent work of Noh and Fernando[19] indicates that the entrainment at density interfaces by mechanically induced shear-free turbulence becomes completely diffusion dominated when Ri exceeds Ri_c, where $\mathrm{Ri}_c \approx 1.6\ \mathrm{Pr\ Pe}^{1/2}$. If this is applicable to the present experiments, the range of Ri_c, for $10^3 < \mathrm{Pe} < 10^4$, would be $350 < \mathrm{Ri}_c < 1120$, which is outside the range of Ri used in the present experiments. The aim of the present experiments was to investigate the influence of molecular diffusion at intermediate Richardson numbers where active turbulent entrainment is taking place, and the characteristics of the completely diffusion-dominated entrainment regime should be investigated in future research.

ACKNOWLEDGMENTS

The authors wish to thank Professor D. F. Jankowski and G. Oth for their help in numerous ways.

The financial support of the fluid mechanics and REU programs of the National Science Foundation and Physical Oceanography and Arctic Sciences Programs of the Office of Naval Research is gratefully acknowledged.

[1] G. E. Willis and J. W. Deardorff, J. Atmos. Sci. **31**, 1297 (1974).
[2] J. W. Deardorff and G. E. Willis, Boundary Layer Meteorol. **32**, 205 (1985).
[3] R. Kumar, Int. J. Heat Mass Transfer **32**, 735 (1989).
[4] J. W. Deardorff, G. E. Willis, and D. K. Lilly, J. Fluid Mech. **35**, 7 (1969).
[5] F. D. Heidt, Boundary Layer Meteorol. **12**, 439 (1977).
[6] L. H. Kantha, in *Fjord Oceanography*, edited by H. J. Freeland, D. M. Farmer, and C. J. Levings (Plenum, New York, 1980), p. 205.
[7] J. W. Deardorff, G. E. Willis, and B. H. Stockton, J. Fluid Mech. **100**, 41 (1980).
[8] J. W. Deardorff in *Workshop on the Planetary Boundary Layer*, edited by J. C. Weil (American Meteorological Society, Boston, MA, 1978), p. 39.
[9] R. E. Breidenthal and M. B. Baker, in *7th Symposium on Turbulence and Diffusion*, edited by J. C. Weil (American Meteorological Society, Boston, MA, 1985), p. 43.
[10] H. J. S. Fernando, J. Fluid Mech. **182**, 525 (1987).
[11] P. F. Crapper and P. F. Linden, J. Fluid Mech. **65**, 45 (1974).
[12] I. A. Hannoun, H. J. S. Fernando, and E. J. List, J. Fluid Mech. **189**, 89 (1988).
[13] S. Narimousa and H. J. S. Fernando, J. Fluid Mech. **174**, 1 (1987).
[14] O. M. Phillips, *Dynamics of the Upper Ocean* (Cambridge U.P., London, 1966).
[15] J. S. Turner, *Buoyancy Effects in Fluids* (Cambridge U.P., London, 1973).
[16] S. Narimousa, R. R. Long, and S. A. Kitaigorodskii, Tellus **38A**, 76 (1986).
[17] J. S. Turner, J. Fluid Mech. **33**, 639 (1968).
[18] E. J. Hopfinger and J.-A. Toly, J. Fluid Mech. **78**, 155 (1976).
[19] Y. Noh and H. J. S. Fernando, EOS **69**, 372 (1988) (also submitted to Dyn. Atmos. Oceans).